Preferred citation: A. Kulachenko, P. Gradin and T. Uesaka. Tension wrinkling and fluting in heatset web offset printing process – Post-buckling analyses. In **Advances in Paper Science and Technology**, *Trans. of the XIIIth Fund. Res. Symp. Cambridge, 2005*, (S.J. I'Anson, ed.), pp 1075–1099, FRC, Manchester, 2018. DOI: 10.15376/frc.2005.2.1075.

TENSION WRINKLING AND FLUTING IN HEATSET WEB OFFSET PRINTING PROCESS – POST-BUCKLING ANALYSES

Artem Kulachenko, Per Gradin and Tetsu Uesaka

Fibre Science and Communication Network (FSCN), Mid Sweden University, Sundsvall, Sweden.

ABSTRACT

Geometrically non-linear, large scale post-buckling analyses were carried out to investigate the influence of different parameters on residual waviness (fluting) after printing in a heat set web offset printing press. Mixed implicit-explicit finite element techniques were used in the analyses. The numerical procedure was verified by experimentally acquired data. Results show that when the paper web is perfectly flat before printing, fluting patterns after drying and moisture recovery generally have higher wavelength than those typically observed in fluted samples. Initial cockles of unprinted sheets were found to have impacts on the fluting patterns and amplitudes. Among the factors investigated, ink thickness and hygroexpansivity had significant influences on fluting: increasing these factors increased fluting amplitudes.

1 INTRODUCTION

Fluting is a print defect that often appears in light-weight, coated and uncoated papers printed in heatset web offset printing processes (Figure 1).

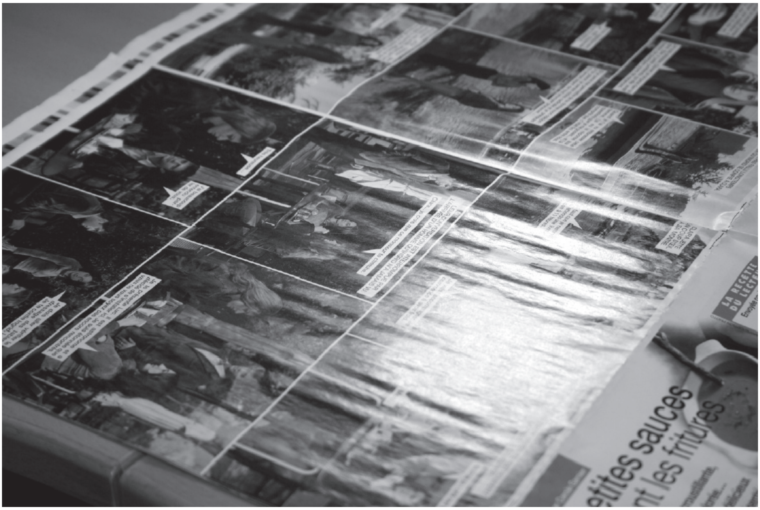

Figure 1 A typical fluting appearance.

Because of its unique corrugated shape along the machine direction (MD), it has been long speculated that some kind of web buckling creates wrinkles, which are later fixed by curing of inks and/or coatings during the drying stage of printing. Accordingly, the question raised among many researchers is what makes the web wrinkle. (In this paper, we distinguish "fluting" from general wrinkling. We define fluting as wrinkling observed in the final printed sheet.)

Habeger [1] started a buckling analysis of a paper web, which is modelled as a shallow shell to capture the essence of tension wrinkle phenomena. Fujiwara [2] proposed the differential shrinkage between the image and non-image areas during printing as a cause of tension wrinkle. Coffin [3] later took the idea and predicted the wrinkle wave length and critical moisture difference for a simplified geometry of a paper web.

An extensive field study of fluting in heatset web offset printing was carried out by MacPhee et al. [4]. Among most significant findings relevant to this study are the following:

- Fluting occurred everywhere in the prints. Fluting in the gutter did however relax to some extent. Visually no variation was seen throughout a given sheet in either amplitude or wavelength.
- A 17 percent decrease in web tension had no visually discernible effect on fluting amplitude.

- Fluting is worsened by an increase in the ink thickness, and less ink-absorbent papers flute less.
- For SC paper, the appearance of wrinkles before and after the dryer was the same and *resembled* the fluting that was present in the final prints. For LWC papers, wrinkles before the dryer bore no resemblance to the tension wrinkles observed beyond the dryer. The latter had typical fluting appearance with average wavelength 1.7–1.8 cm.
- Open flame (impingement) dryers, with smaller web heat-up, generally do not have a fluting problem.

These studies provided a number of important insights on the basic mechanisms of wrinkling in the printing process. However, the results are still not able to quantitatively predict “fluting” in a printed sheet. One of the main challenges is that the investigation of fluting requires a “post-buckling” analysis, i.e., the analyses of the buckling incident as well as subsequent changes in the buckled shape (amplitude and wave length). In addition, the complexity of the entire mechanical/moisture/temperature histories to which the paper is subjected in the heatset web offset printing processes poses another challenge.

The overall objective of this study is to identify key paper factors and printing process variables that control the fluting *amplitude* and wave length of the web after heatset offset printing. To achieve this objective, it was decided to develop finite element analysis procedures that allow the *post-buckling* analysis. Using this procedure, we investigate the basic mechanics, and design critical experiments that will confirm the mechanisms hypothesised in numerical analyses.

In this paper, the main objectives are to develop the finite element procedures, to verify the numerical methods with controlled experiments, and then to perform parametric studies for the effects of different factors of papers, such as bending stiffness, moisture change, and hygroexpansion coefficients, as well as boundary conditions related to the printing press.

2 EXISTING APPROACHES TO MODELLING FLUTING

2.1 Buckling analysis

Paper constitutes a very thin material and it easily buckles under compressive forces. In the case of fluting these compressive forces obviously develops in the cross direction (CD). If there are no constraints and paper is perfectly uniform and flat, the compressive stresses may not appear. This follows explicitly from the boundary conditions.

One of the most popular approaches to study wrinkling or fluting of a paper web has been a linear buckling analysis which may be carried out by finite element method (FEA) as well. It has certain limitations and the most noticeable are

- inability to account for any type of nonlinearity, either material or geometrical;
- a structure must be assumed to be linear elastic and such phenomena like moisture change that might alter material properties of the web cannot be accounted for;
- inability to predict post-buckling deflections.

The linear buckling theory often results in overestimating the buckling strength. Furthermore when the linear buckling theory is applied to a flat, constrained, extremely thin paper sheet which is subjected to tension, the first mode of buckling occurs at comparatively low tension. They are followed by "noisy" modes that come one after another in a dense sequence. It is therefore impossible to identify the real modes and predict which mode will occur in reality. A simple example – a buckling analysis with a finite element method of a 70 μm thick, 4 × 1.5 m constrained isotropic plate with elastic modulus 10 GPa and Poisson's ratio 0.3, subjected to uniform tension results in the following critical tensions (sorted by the shape number): 26.8, 41.3, 57.9, 76.12, 96.18, 118.19 N/m, etc. Without some assumptions, it is hard to predict how these modes will be superimposed at, say, 300 N/m.

2.2 Post-buckling analysis

Non-linear buckling analysis is usually a more accurate option. This technique employs a non-linear analysis with gradually increasing loads and enables one not only to determine the buckling forces but also to track the post-buckled performance of a structure. In order to avoid a sharp bifurcation in the load-displacement curve, structures such as flat sheets, cylinders, and spheres must either have some imperfection built into the original geometry or have it created by an initial preloading.

A solution of non-linear partial differential equations by FEA depends on the specific finite element technology used and the methods for solving the equations. In the context of FEA, membrane elements or shell elements can be used to discretize the model of a paper web. Membrane elements do not have any bending stiffness and hence convergence might not be achieved in the presence of local instabilities such as wrinkling. On the whole, modelling of wrinkling is much simplified when bending stiffness is introduced in the model with the use of shell elements. There are a variety of shell elements based on different kinematic assumptions. From the literature [5, 6] and the authors' experience, the most robust shell element in non-linear finite element analyses is one based on the Mindlin-Reissner Shell Theory (MRST) which treats the rotations as separate variables not dependent on displacement, contrary to the classical shell theory. Thin shells modelled with MRST introduce additional problems such as shear and membrane locking [7]. There has been much effort made to cope with these problems and most of the modern commercial finite element codes have efficient and robust shells of this kind. For extremely thin shell elements the bending stiffness is much smaller than the membrane stiffness. This may cause ill-conditioning of both the element and the global stiffness matrix.

Modelling of fluting requires a quasi-static post-buckling analysis. There are two general approaches for solving quasi-static problems in FEA [8] which differs in time integration schemes: *implicit* and *explicit*. The difference can be shown on a general Newmark-type integration where the following interpolation at a time step n is employed:

$$\begin{aligned} \mathbf{M}\ddot{\mathbf{u}}_{n+1} + \mathbf{C}\dot{\mathbf{u}}_{n+1} + \mathbf{K}(\mathbf{u}_{n+1}) &= \mathbf{F}(t_{n+1}) - \mathbf{R}(\mathbf{u}_{n+1}) \\ \mathbf{u}_{n+1} &= \mathbf{u}_n + \Delta t\dot{\mathbf{u}}_n + \Delta t^2[(0.5 - \beta)\ddot{\mathbf{u}}_n + \beta\ddot{\mathbf{u}}_{n+1}] \\ \dot{\mathbf{u}}_{n+1} &= \dot{\mathbf{u}}_n + \Delta t\,[(1 - \gamma)\,\ddot{\mathbf{u}}_n + \gamma\ddot{\mathbf{u}}_{n+1}] \end{aligned} \tag{1}$$

where **M** is the mass matrix; **C** is the damping matrix; **K** is the stiffness matrix, $\mathbf{u}$, $\dot{\mathbf{u}}$, and $\ddot{\mathbf{u}}$ are the displacement, velocity and acceleration vectors; **F** is the vector of external time dependent forces; **R** is the vector of internal forces; Δt is the time step; β and γ are the integration parameters.

In the *implicit integration* scheme the values sought are displacements, and the integration parameter in a standard Newmark scheme are $\beta = 0.25$ and $\gamma = 0.5$. The stiffness matrix has to be inverted to solve Equation (1) at a given time step. In a non-linear analysis, Newton-Raphson iterations are performed to find a solution for load step increment. Although the stiffness matrix is usually sparse, this process is still computationally intensive and requires considerable memory resources. When the structure undergoes instability, the stiffness matrix possesses singularities and it is hard to obtain a converged solution. Wrinkling is a local instability which is indicated by sudden convergence difficulty even with very small load step increments in the implicit analysis. Sometimes it may not be possible to obtain a static solution with implicit methods in the presence of local instabilities and then an explicit method is a possible option.

For the *explicit solution* one solves for accelerations first. The integration parameters are set to $\beta = 0$ and $\gamma = 0.5$ which results in a second-order central difference scheme. That is, when the mass and damping matrices are diagonalized, the solution may be found quickly because inversion of diagonal matrices is a trivial operation. No iteration is required at a given time step. The significant drawback of this method is the fact that this integration scheme is only conditionally stable. Contrary to the implicit method, where the time step can be of arbitrary size and rather dictated by loading characteristics, the explicit method uses the time step dictated by the physical characteristics of the finite element model such as element size, stiffness, and mass. A time step size for a given element must be smaller than the time it takes for a stress wave to travel across the element (Courant stability criteria [7]). The smaller the element size is, the smaller the time step becomes. Thus one requires, among other things, time-efficient elements (e.g., based on reduced integration) to complete the calculations with a dense mesh in a reasonable time. Moreover, there are some ad hoc methods to achieve artificial speed-up:

- to increase the loading rates. It should be noted that to make the simulation quasi-static, the loading rates must be such that the kinetic energy remains small compared to the internal energy throughout the analysis. (An accepted value is less than 1%.);
- to scale the mass of the model.

Both have the effect of increasing the time increment needed for a stable solution process. Most shell elements in the explicit codes are made to be computationally cheap by using reduced integration schemes. Their performance and accuracy must therefore be examined afterwards regarding a set of various output parameters, benchmark tests with different mesh densities and artificial parameters involved in the element formulation.

In this study, these integration techniques were used interchangeably.

3 EXPERIMENTAL VERIFICATION

Since there is no analytical solution available to check the applicability of FEA for simulation of post-buckling behaviour of extremely thin shells, it was decided to conduct a well defined experiment using a thin aluminium foil. The foil (60 × 30 cm and 10 μm thick) was subjected to tension by means of wide grips, until wrinkles developed. In order to obtain a uniform distribution of the pressure from the grips the ends of the foil were placed between wooden bars. A laser displacement sensor (MEL/M7, Mikroelektronik GmbH) was utilised for precision measurements of the out-of-plane displacements as shown in Figure 2. The elastic constants were determined for

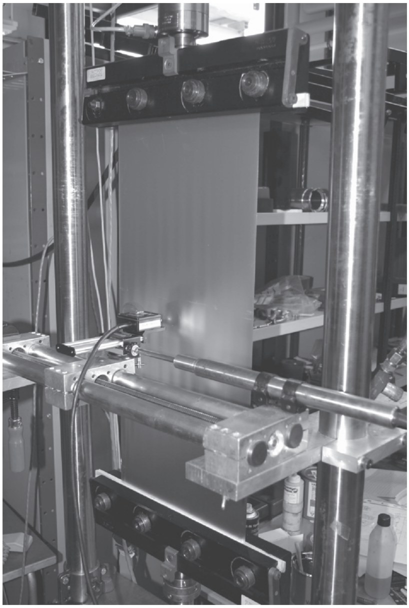

Figure 2 Experimental setup.

the foil sample. Several trials were carried out in order to obtain a symmetric wrinkling pattern, which would indicate that the load is distributed uniformly across the width.

The LS-Dyna 970 (Revision 5434, double precision version) commercial finite element code was utilised in this work [9]. A Total Lagrangian formulation was used to solve the non-linear continuum equations. The FE-models were meshed with the 4-node, Belytschko-Wong-Chiang, under-integrated elements [10]. Static implicit integration method was used during preloading and switched to the explicit integration technique when computing the post-buckling part. This made it possible to perform preloading in one load step and to avoid sudden energy explosions in the transition between the loose and stretched web at a high loading rate. The models were stretched and gravity was applied to initiate a small out-of-plane perturbation. The artificially high loading rates were used to speed up the analysis. When the wrinkles developed, at the final stage of the analysis, global mass-proportional damping was introduced to eliminate small oscillations near the final state. This stage in a quasi-static analysis is called Dynamic Relaxation. Choosing a CPU efficient global damping parameter requires some trial-and-error efforts

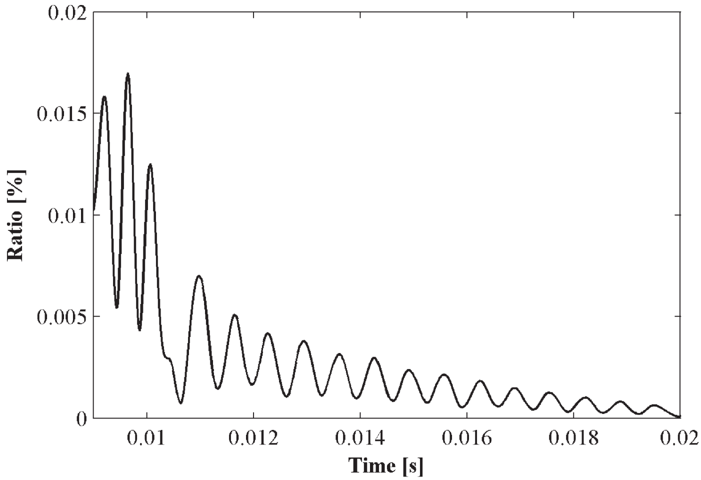

Figure 3 Ratio between kinetic and internal energies during the explicit stage of the analysis.

because it should not "freeze" the structure but allow the vibrations to relax in a shortest time possible. In spite of high loading rates the relation between the kinetic and internal energies stayed in the permitted range (<<1%) (Figure 3).

The under-integrated shell elements, although being free of the locking problems, are known to possess spurious or "hourglass" energy modes [11]. To circumvent this problem the hourglass control was used which introduces small artificial forces and stiffnesses which would help in resisting spurious deformations. The contribution of these members to the total energy must be carefully controlled. If the ratio of the artificial energy to the total energy is less than 5%, the solution is generally acceptable. In this problem this ratio stayed far below this limit (Figure 4).

Considering the fact that the experimental sample still possesses considerable imperfections, such as curl, we found that the comparison yielded a reasonable correlation between the FEA predictions and measurements in terms of wavelength and amplitudes (Figure 5).

A similar analysis was carried out with the reference to the experiments done by Land [12], in which a deflection profile of a part of the web was captured by CCD camera. Except the exact locations of the wrinkles, simulation results showed a good prediction of the magnitude and wavelength of the wrinkles (Figure 6).

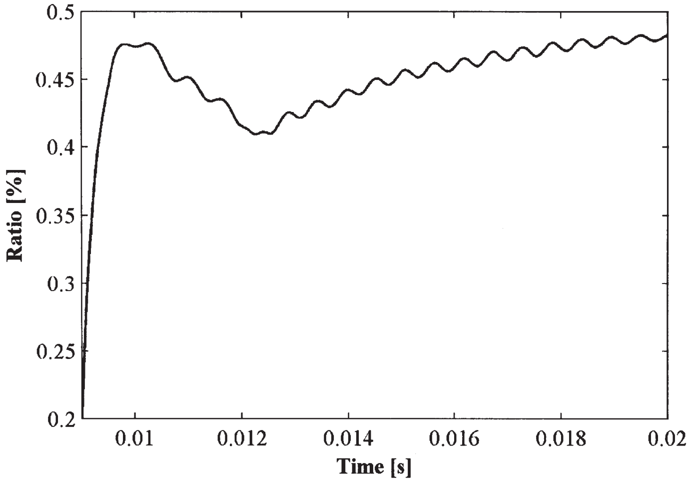

Figure 4 Ratio between hourglass resistance and total energies during the explicit integration stage of the analysis.

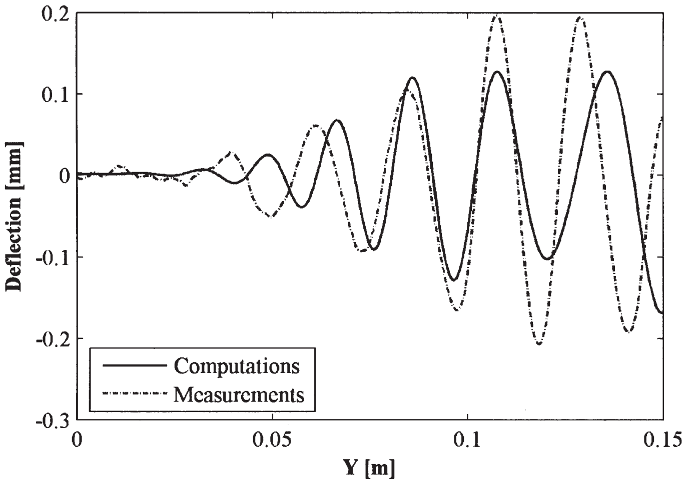

Figure 5 Comparing the FEA predictions with the measurements.

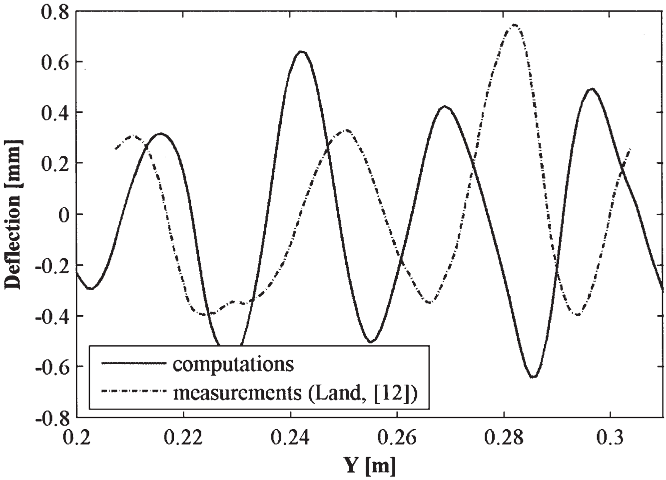

Figure 6 Comparing the FEA predictions with the measurements from the reference [12].

4 RESULTS AND DISCUSSIONS

4.1 Boundary conditions and model parameters

The boundary conditions to which the web is subjected in the span between two sets of rollers have always been a matter of discussion among researches. It is expected that the real boundary conditions are somewhat between the unconstrained and constrained states as the web may adapt to CD deformations on the way from one roller to another. In the analyses that follow, the reference problem (control) will be the web which is not constrained in CD. For the parametric study of the post-buckling behaviour we chose a 4-meter long and 1.5-meter wide web with an image layout as shown in Figure 7. Image areas are depicted by shaded areas.

4.2 Parametric studies

4.2.1 Wrinkling at the moisture uptake stage

Moistening during printing through inks and fountain solutions was considered under the following assumptions:

- the web is stationary;
- hygroexpansion coefficients are independent of moisture;

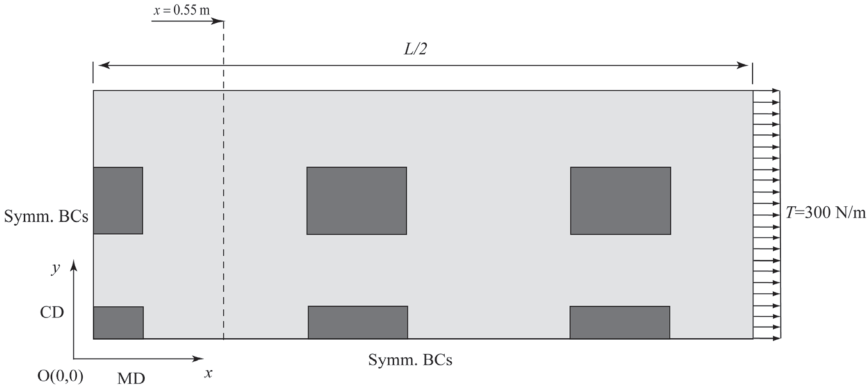

Figure 7 Problem for the parametric study.

- the image areas pick up 4% of moisture content while the rest of the web takes up only 2%;
- the hygroexpansion coefficients were assumed to be 0.05 in the MD and 0.15 in the CD (% deformation/% moisture content change);
- the moisture is uniformly picked up in the z-direction and does not cause thickness swelling.

The moisture absorption levels were chosen based on the work of Hansen [13], and the data for orthotropic elastic properties as a function of moisture content of the paper web were similar to those used in the literature [12]. Out-of-plane displacements were output from the nodes located in the cross section at x = 0. Tension was uniformly distributed at the boundaries and remained constant throughout the analysis. The element size was 0.3 mm. The deformed web is shown in Figure 8.

The output parameters were monitored in a similar way to what is described the verification test. Besides, it is worth saying that the element size was 0.3 mm. The size of 0.15 mm was also tested for the reference problem and it resulted in only an insignificant shift of waviness.

Effects of thickness (bending stiffness)

The thickness was increased by a factor of 2 which consequently gave an 8 times larger bending stiffness. Surprisingly, this had little influence on the overall picture. The wavelength increased but the amplitude stayed nearly the same and even grew slightly in the image area (Figure 9a). Therefore, in the *moisture application stage* (before drying), higher bending stiffness does not have a positive effect for preventing web wrinkles.

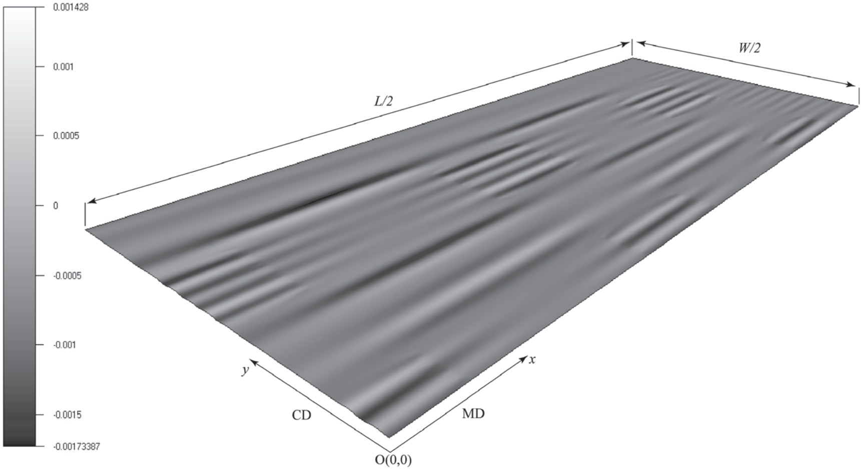

Figure 8 Out-of-plane deformations of the web.

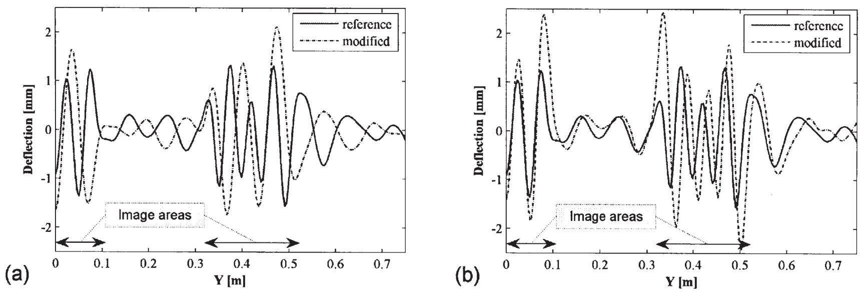

Figure 9 Wrinkling profiles: (a) increased thickness by a factor of 2; (b) increased hygroexpansion coefficient by a factor of 2.

Hygroexpansion coefficient

Increasing the CD hygroexpansion coefficient by a factor of 2 increased the amplitudes, particularly in the image areas, but did not affect the wavelength significantly (Figure 9b).

Tension

Decreasing the tension by a factor of 2 slightly shifted the wrinkle pattern, but the amplitude and wave length did not change significantly (Figure 10a).

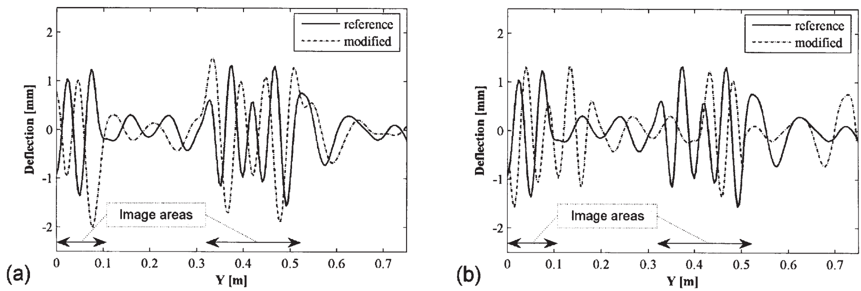

Figure 10 Wrinkling profiles: (a) decreased tension by a factor of 2; (b) increased web length by a factor of 1.5.

Web length

Increasing the web length, with the same element size, redistributed the wrinkle patterns, but the maximum amplitudes were not influenced greatly (Figure 10b).

Moisture pick-up

As expected, decreasing the moisture pick-up by a factor of 2 reduced the amplitudes in both image and non-image areas (Figure 11a). (Note that moisture pick-up affects both hygroexpansion strains and paper stiffness. Therefore, the effect is not the same as the effect of changing hygroexpansion coefficients.)

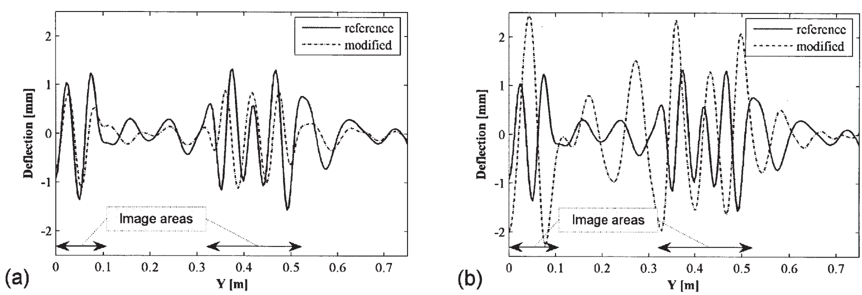

Figure 11 Wrinkling profiles: (a) decreased moisture pick-up by a factor of 2 (left); Added constraints in the CD (right).

Constraints in the CD at the boundaries

The constraints in the CD increased the amplitudes considerably. The effect was comparable with that of the moisture-related changes. Furthermore, they increased the amplitudes in the non-image areas (Figure 11b).

The most important observation from the analyses of the moisture uptake stage is that the wave length of wrinkles are generally in the range of 7–10 cm, which is significantly higher than the typical fluting wave length (~1 cm) observed in heatset web offset printed sheets. This raises a fundamental question of whether the tension wrinkles are the same as fluting in printed sheets.

4.2.2 Fluting after drying stage

The following assumptions were made to construct a reference problem as to the drying process:

- moisture content is uniformly reduced over the non-image areas by 3%;
- the image areas loose less moisture, 2%, since the ink prevents evaporation [2];
- the ink layer is 1 μm thick and can be represented by an isotropic material;
- the ink layer becomes stiff before moisture recovery starts after drying;
- at the final state the web restores its initial moisture content throughout the web.

The two following hypotheses were made as to ink solidification.

Hypothesis 1: Ink starts to solidify only at the chilled roll position, and "quickly" ends solidification. It is therefore assumed that at a high temperature, chemical components of the ink do not form a stiff layer on the web surface. Ink was introduced on the deformed web at the end of the drying without initial stress and strains. The computations were interrupted just before the solidification point; the shell elements representing the web are overlaid by ink elements that have their nodes coincident with the deformed web elements. The ink material of the ink is chosen to be elastic and temperature dependent. This material has small elastic modulus E_{T_1} at the temperature T_1 and large elastic modulus E_{T_2} at a temperature T_2.

Hypothesis 2: Ink starts solidifying as soon as drying starts and ends at the end of drying process (at the chilled roll position). It means that ink has a zero strain state at the initial configuration. An ink element constituted a three-layered shell. Two surface layers are thin and have ink material properties. A middle layer has dummy material properties and does not contribute to the ink thickness. Ink elements were connected through the tied

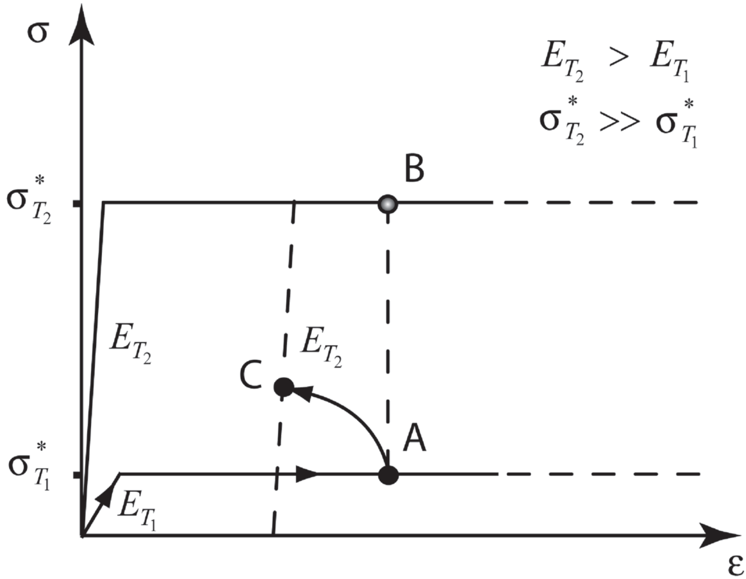

Figure 12 Ink material model.

surface-to-surface contact algorithm with force and moment transfer. The ink material was chosen to be ideally elastic-plastic and temperature dependent. At a temperature T_1 this material has small elastic modulus E_{T_1} and extremely small yield stress $\sigma^*_{T_1}$, so that it becomes plastic at a very low stress and provides almost no resistance to the deformation. At a temperature T_2, on the other hand, it has high elastic modulus E_{T_2} and yield stress $\sigma^*_{T_2}$. Therefore, when the temperature changes to T_2, the material becomes stiff and has initial strains developed while it was plastic at the temperature T_1. This material behaviour is illustrated in Figure 12.

If, during the temperature changes, the constant strain is maintained, in this simple uniaxial example, the material will come to point B. When the ink is attached to another element, the material will rather arrive at a point C having some unrecoverable deformation. From the point C it will respond elastically.

In the simulations the following material properties were assigned to the ink elements:

$$E_{T_1} = 1 \text{ MPa} \qquad \sigma_{T_1} = \text{Pa}$$

$$E_{T_2} = 30 \text{ GPa} \qquad \sigma_{T_2} = 1\ G\text{Pa}$$

Table 1 Loading parameters.

Case	Tension [N/m]	MC [%]. NIA	MC [%]. IA	Mechanical damping [*]	Ink [*]	Explicit (E) / Implicit (I)
1	0	8.4	8.4	0	1/0**	I
2	400	8.4	8.4	0	1/0**	E
3	400	5.4	6.4	0	1/0**	E
4	400	5.4	6.4	1	1/0**	E
5	400	5.4	6.4	0	1	E
6	400	8.4	8.4	0	1	E
7	0	8.4	8.4	1	1	E

MC – moisture content
IA – image area
NIA – non-image are
* – [0-disabled; 1-enabled]
** – ink solidification method (1) / method (2)

Ultimate ink stiffness was chosen from a feasible range presented in [14] so that the bending stiffness in the image area with ink thickness of 1 μm is increased approximately by 25%, as it is stated in [15]. (Note that the ink thickness was not given in this reference.)

A loading process was partitioned onto the 7 steps where parameters are changed according to Table 1.

All parameters are interpolated linearly between the steps. It should be noted that this loading schedule does not include the moisture uptake stage that was discussed earlier. This is because as soon as drying starts after printing, the web reaches the stage 3 (Table 1) in an elastic manner and therefore the final results are the same as in the case of the loading schedule in Table 1. The moisture was restored under tension simply to prevent the unconstrained motion, when displacements in MD are solely driven by internal forces. This should not influence the result because all the materials are in elastic region as soon as the moisture recovery begins.

The cases considered in this section are described in Table 2.

The following terms are used:

Plane – initially plane paper web

Cockled – paper web with periodical cockles along the length. Cockling wavelength in the CD is specified in Table 2, maximum cockling amplitude h_c is 100 μm [16]. Cockles are defined by the function

Table 2 Cases for the drying process simulations.

Case	Geometry / cockle wavelength (if applicable)	Paper thickness [µm]	Ink thickness [µm]	Solidification hypothesis	Hygroexpansion coefficients
1	Plane	62.3	1	1	Normal
2	Plane	62.3	3	1	Normal
3	Cockled / 1 cm	62.3	1	1	Normal
4	MD cockle / 2 cm	62.3	1	1	Normal
6	MD cockle / 1 cm	62.3	1	1	Normal
6	Plane	62.3	1	1	Decreased
7	Plane	82.3	1	1	Normal
8	Plane	62.3	1	2	Normal

$$z_c\,(x,y) = h_c \sin^3(x) \cos(y)$$

where x is the MD coordinate and y is the CD coordinate. Cubic dependence on the MD coordinate was chosen to ensure a zero derivative at the start and end of the cockled regions along the MD. Length of the cockled regions (half-wave length of $\sin^3(x)$) was 15 cm; the distance between the cockled regions was 1 cm. Note that the actual length of the cockled region will look shorter than 15 cm due to the behaviour of the function $\sin^3(x)$.

Cockle MD – paper web with continuous cockles along the MD. The cockling wavelength in the CD was chosen to be 1 cm and 2 cm, and the cockling amplitude is 60 µm.

Figure 13 shows an example of cockles of an unprinted sheet. The simulation of the effects of cockles of unprinted sheets was motivated by the fact that every paper has cockles to different extents and the web stability is known to be sensitive to initial imperfection.

With the proposed loading scheme, a web without ink must restore its original shape in the end of analysis. This case was used for tuning dynamic relaxation parameters. The maximum deviation from the original plane state with the final dynamic relaxation settings used was 3 µm which is a good resolution for this type of problem.

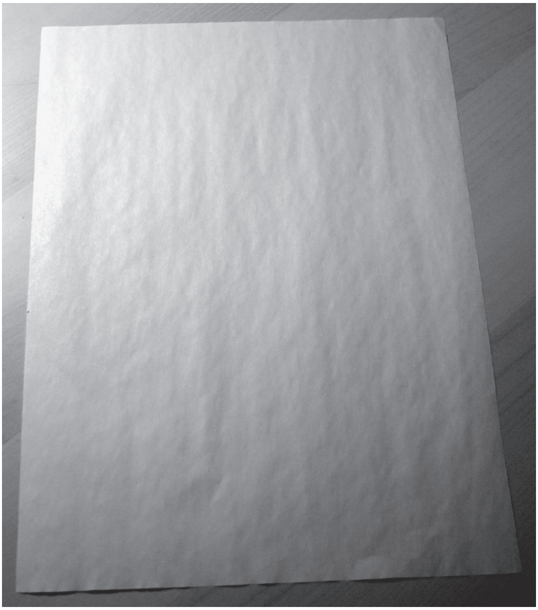

Figure 13 An example of cockling appearance.

Case#1 (Plane web, the reference case)

Figure 14 shows deflection profiles in the CD for the reference case. The left-hand figure shows a profile at x = 0 (the centre of the web, as seen in Figure 7), and the right-hand figure shows a profile at x = 0.55 m (as indicated by a broken line in Figure 7). Figure 15 shows a corresponding deformation picture.

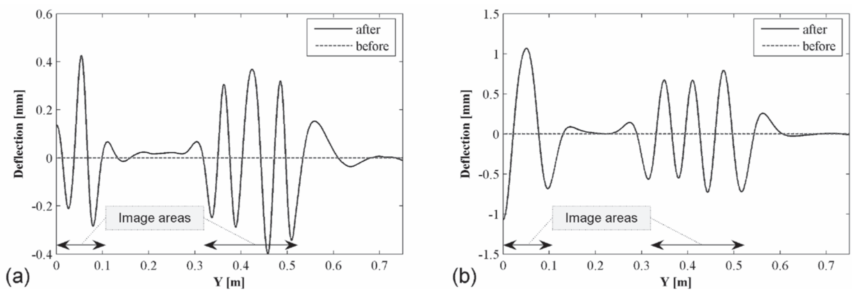

Figure 14 Case#1. Profile (a) at x = 0; (b) at x = 0.55 m.

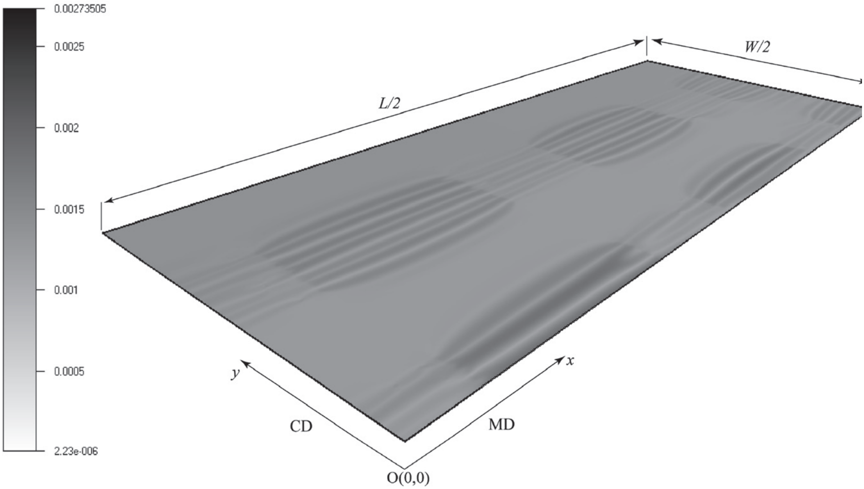

Figure 15 Case#1. Out-of plane deformation of the web.

The fluting pattern received in this case was, again, far from those typical for fluting: the wave length in the image areas is in the order of 10 cm, much larger than a few centimetres. The wave amplitudes and wave lengths across the non-image regions (x = 0.55 m) were higher than those across the image regions.

Case#2 (Plane web, increased ink thickness)

In this case ink thickness was increased from 1 μm to 3 μm. Comparing the results with those for the reference, one finds that increasing ink thickness increases the amplitudes, particularly in the image areas. This result fits to the field observation that fluting is more frequently seen in heavily ink-covered areas [1, 15].

Under the simulation condition used in this study, it is possible to say that ink influences the amplitudes of residual distortion significantly (see Figure 16).

Case#3 (Periodically cockled web. Cockling wavelength is 1 cm)

Figures 17 and 18 show deflection profiles across the non-cockled and cockled region, respectively. For this periodically cockled paper, the global buckling modes, as seen in the reference case with 8–10 cm wavelength and 0.3–0.5 mm amplitude, were dominant in the solution, while initial cockling

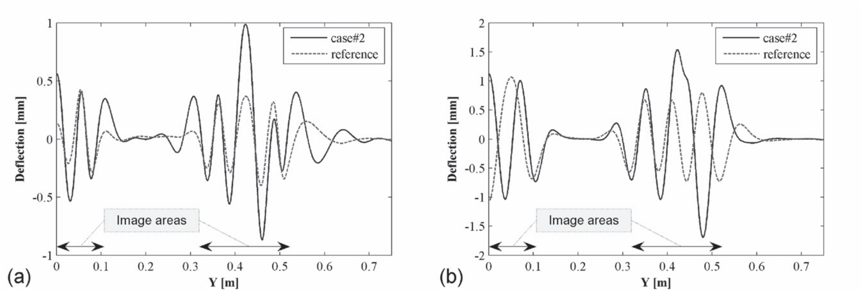

Figure 16 Case#2. Profile (a) at x = 0; (b) at x = 0.55 m.

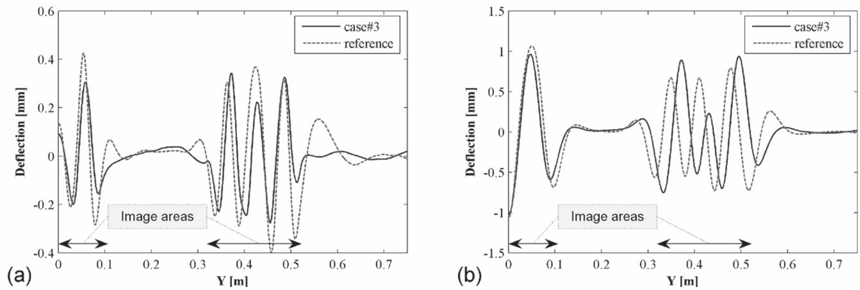

Figure 17 Case#3. Profile across non-cockled regions (a) image area (b) non-image area.

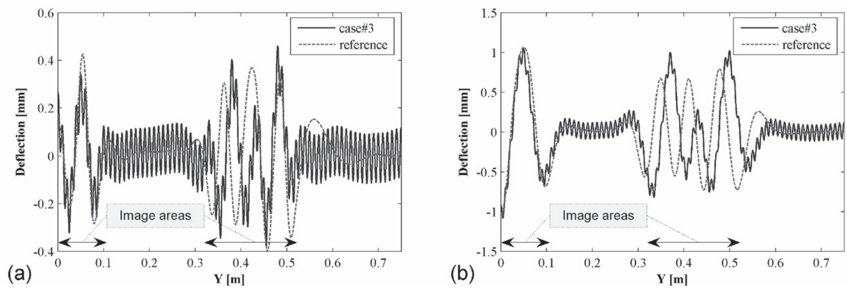

Figure 18 Case#3. Profile across cockled regions (a) image area (b) non-image area.

remained in its original locations with the same amplitudes. Cockles introduced on geometry level did not significantly propagate further along the web into the non-cockled regions. In general initial cockling and global buckling were superimposed without any interaction. This is probably because the wave lengths are distinct from each other. The wavelengths and amplitudes did not change much in comparison with those for the reference case.

These high-frequency, cockle-originated flutes in Figure 18 may show up in a very distractive way in a magazine-size paper when the paper is printed and gloss is enhanced.

Case#4 (MD cockle. Cockling wavelength is 2 cm)

In this case, initial cockling with a relatively long wavelength 2 cm and small 60 μm amplitude interacted with the global buckling mode (Figure 19). The initial cockling was smoothed in the buckled areas, but it created new, very high peaks in the web centre region (x = 0, Figure 19a).

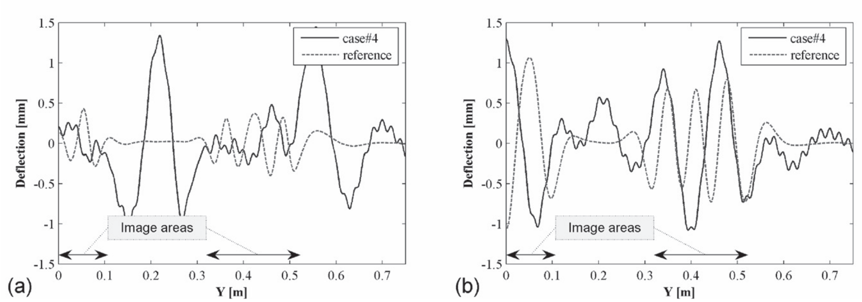

Figure 19 Case#4. Profile (a) at x = 0; (b) at x = 0.55 m.

Case#5 (MD cockle. Cockling wavelength is 1 cm)

As seen in Figure 20, the initial cockling shape in the image areas remained almost unchanged but created new high peaks in the non-image areas.

These results from the simulations for Cases 3, 4, and 5 clearly indicate that initial cockling of unprinted sheets has great impacts on both fluting patterns and amplitudes, and the wavelengths of the initial cockles in the MD and CD are a critical factor.

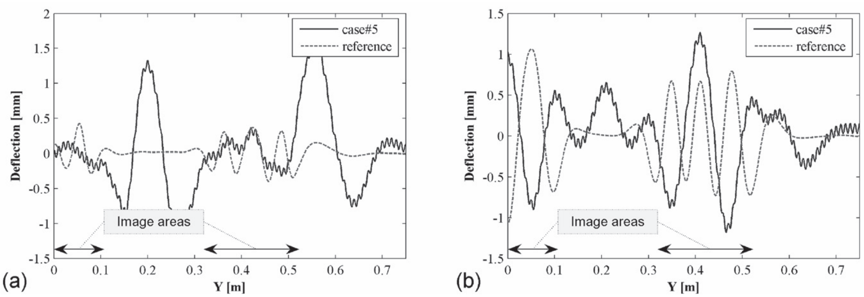

Figure 20 Case#5. Profile (a) at x = 0; (b) at x = 0.55 m.

Case#6 (Plane web and decreased hygroexpansivity)

Decreasing hygroexpansivity by 50% decreased the amplitudes of fluting in the global buckling mode, to some extent. This result is similar to that for the moisture uptake simulation discussed earlier (see Figure 21).

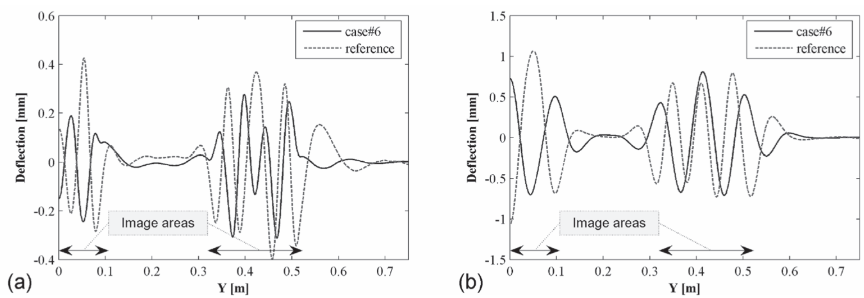

Figure 21 Case#6. Profile (a) at x = 0; (b) at x = 0.55 m.

Case#7 (Plane web, increased paper thickness by 30%)

Surprisingly, again, decreasing paper thickness by 30% did not affect the fluting amplitudes significantly. The field observations [e.g., 15] often claim that thicker grade papers flute less as compared with thinner grades. The result obtained here poses a fundamental question of whether such behaviour is due to the difference in the buckling response during printing or the difference in the initial cockling (see Figure 22).

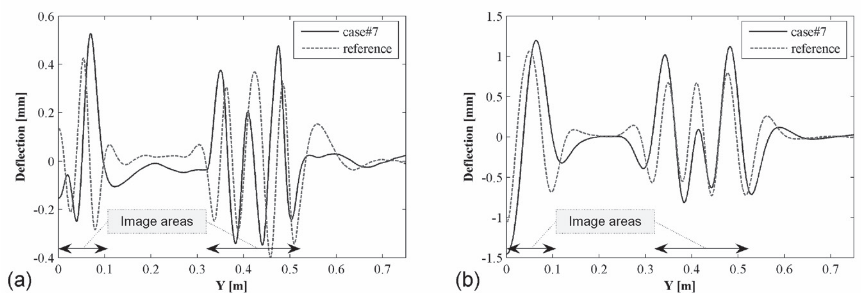

Figure 22 Case#7. Profile (a) at x = 0; (b) at x = 0.55 m.

Case#8 (Ink solidification method. Hypothesis 2)

Interestingly changing the ink solidification scheme altered the deflection pattern drastically: this hypothesis removed most of fluting. It is still unclear whether this is an effect of ink solidification histories or an influence of the chosen ink material model. This particular case will be given a closer attention in subsequent studies (see Figure 23).

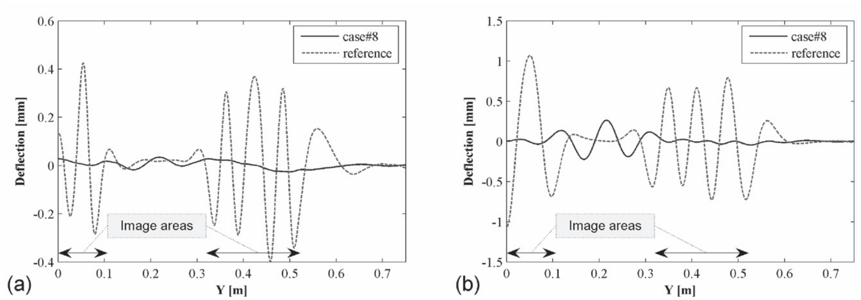

Figure 23 Case#8. Profile (a) at x = 0; (b) at x = 0.55 m.

5 CONCLUDING REMARKS

In the moisture uptake stage, an unexpected result was obtained from this parametric study. The bending stiffness had little influence on wrinkling, while the CD constraints showed a great effect on the wrinkle amplitude. Altering moisture-related parameters led to expected results. No significant influence of the tension and the web length was revealed. Most importantly, the fluting wavelength (in the order of 6 cm) appeared in the simulations was consistently higher than the ones for the fluting often observed in the printed sheets (approximately 1 cm or even less). The amplitudes were higher as well. Apparently the pure *moistening* is not the main reason of the usually-observed fluting.

In the drying stage, "fluting", residual wrinkles after drying and moisture recovery, appears in our simulation by introducing ink and its solidification. For initially flat papers, the wavelengths of flutes were in the range of 6 cm to 10 cm. As one introduces initial cockling to the unprinted sheets, the flute patterns changed. High frequency (small wave length) cockles tend to remain in the original locations and retain their amplitudes even after printing, drying and reconditioning. Longer wave-length cockles, on the other hand, tend to interact with the global buckling modes. They are sometimes diffused, and sometimes create new flutes with very high amplitudes. The fluting with the wave length of about 1–2 cm often seen in printed sheets are, therefore, likely to originate from initial cockles of unprinted sheets, or driven by the same mechanism that creates them (e.g., non-uniform drying in a few millimetre scale). Among different factors that affect fluting patterns and amplitudes, ink thickness and hygroexpansivity had significant impacts: increasing these factors increased fluting amplitudes. The effect of local moisture variations on fluting will be reported in the subsequent paper.

ACKNOWLEDGEMENTS

The financial support from PrintTech Research programme T2F is greatly acknowledged. Authors acknowledge Cecilia Land at STFI-Packforsk AB who kindly provided data and useful notes regarding the topic of this article.

REFERENCES

1. C.C. Habeger. Tension wrinkling and the fluting of light-weight coated papers in web-offset printing. *Journal of Pulp and Paper Science*. **19**(5):214–218, 1993.
2. S. Fujiwara, T. Fukui, and T. Hirabayashi. Factors of the Fluting of Coated Paper in Web-offset Printing. In proc. *1998 Pan-Pacific and International Printing and Graphic Arts Conference*, pp52–57, JTAPPI, Quebec City, 1998.
3. D. Coffin. A buckling analysis corresponding to the fluting of lightweight coated webs. In proc. *International Paper Physics Conference*, pp31–36, Victoria, B.C., Canada, 2003.
4. J. MacPhee, V. Bellini, B.E. Blom, A.D. Cieri, V. Pinzone and R.S. Potter. **The**

effect of certain variables on fluting in heatset web offset printing. Web Offset Association, Affiliate of Printing Industries of America Inc, 2000.
5. R.H. MacNeal. Perspective on finite element for shell analysis. *Finite Elements in Analysis and Design*. **30**:175–186, 1998.
6. T.Y. Yang, S. Saigal, A. Masud and R.K. Kapania. A survey of recent shell finite elements. *International Journal for Numerical Methods in Engineering*. **47**(1–3): 101–127, 2000.
7. T. Belytschko, W.K. Liu and B. Moran. **Nonlinear Finite Elements for Continua and Structures**. John Wiley and Sons, 2000.
8. K. Schweizerhof, M. Walz, W. Rust, U. Franz and M. Krichner. Quasi-static structural analysis with LS-DYNA – Merits and Limits. In proc. *2nd European LS-DYNA User's Conference*, Gothenburg, Sweden, 1999.
9. J.O. Hallquist. **LS-DYNA. Theoretical Manual**. Livermore Software Technology Corporation, 2001.
10. T. Belytschko, B.L. Wong and H.-Y. Chiang. Advances in one-point quadrature shell elements. *Computer Methods in Applied Mechanics and Engineering*. **96**:93–107, 1992.
11. T. Belytschko, J.S.-J. Ong, W.K. Liu and J.M. Kennedy. Hourglass control in linear and nonlinear problems. *Computer Methods in Applied Mechanics and Engineering*. **43**:251–276, 1984.
12. C. Land. Effect of moisture amount on HSWO waviness. In proc. *International Printing and Graphic Arts Conference*, Vancouver, Canada, 2004.
13. Å. Hansen. Water absorption and dimensional changes of newsprint during offset printing. In proc. *Taga/IARIGAI Conference*, Hilton Paris, France, 1995.
14. K. Kohno, MHI research and development activities on paper deformation in paper machines. Presentation at Pulp and Paper Research Institute of Canada, 7 August, 1989.
15. Mead Corp. Paper distortion from heatset web offset printing. Mead Corp. Graphics Arts Bulletin No. 11, 1984.
16. I. Kajanto. Finite element analysis of paper cockling. *Trans. 10th Fund. Res. Symp. British Paper and Board Maker's Ass.*, Oxford. **1**:237–262, 1993.

Transcription of Discussion

TENSION WRINKLING AND FLUTING IN HEATSET WEB OFFSET PRINTING PROCESS – POST-BUCKLING ANALYSES

Artem Kulachenko, Per Gradin and Tetsu Uesaka

Fibre Science and Communication Network (FSCN), Mid Sweden University, Sundsvall, Sweden.

Peter Herdman Arjo Wiggins Ltd

There is a reference that you probably would not easily come across by L. Mahadevan (L. Mahadevan *et al*. Nature Vol 419, 10 Oct 2002, p579. See also http://www.deas.harvard.edu/softmat/publications/25.pdf) who was a professor here at Cambridge and is now working at Harvard. He did some work on wrinkling, not of paper structures, but of all film materials including aluminium foils, plastics and textiles. From purely geometric considerations, he observed that if you make a planar strain on a flat material, you produce flutes of a very precisely defined wavelength and the wavelength comes out as an extremely simple equation. The wavelength, λ, is equal to the square root of the thickness of the film material, t, multiplied by the length, L, between the two constraining zones. Now, if for example, it was two clamps, as with your aluminium foil, it is easy to understand the characteristic distance as the distance between the clamps. My hypothesis is that when you are seeing this type of phenomenon with printing, possibly it is the distance between two wet inked areas on the paper or two other types of constraints in the paper. If you try this equation out ($\lambda \approx (tL)^{1/2}$) those phenomena are driven by strain alone and it is a geometrical consideration.

Artem Kulachenko

Thank you very much for the comment. We are aware of such references, but we think that you cannot describe post-buckling phenomena with an equation because, when the paper wrinkles, you are already looking at some other structure, which is not the same that we initially considered. Another point is that tension wrinkles are not supported by practice. If you talk to printing people, they know that some papers flute and some do not. It was possible to show that tension wrinkles are not the cause of fluting. We are very confident about that.

Tom Lindström STFI-Packforsk AB

During the first day here, we discussed extensively flow instabilities in headboxes. Can we rule out that those streaks that we usually find in sheets are behind these phenomena?

Artem Kulachenko

As I said, we are currently investigating the main cause of strain variations because we believe this is the phenomenon behind fluting. We have not found it and thus have not concluded, what it is exactly. So, I cannot answer this question right now, but it was shown that many beautiful papers without any streaks show fluting.

Doug Coffin Miami University

For the post-buckling analysis, your end state is when the moisture has come back to equilibrium again. That takes a long time measuring samples and the observations are that fluting is reduced over the time, but over that time there is also a lot of relaxation going on so you never get back to the flat sheet. So I do not see how it contradicts the hypothesis that differential moisture could cause the fluting and if everything was reversible, it would come out when the moisture equilibrated.

Artem Kulachenko

But in our case, we have ink introduced on paper so we might expect some wrinkles to remain on the web. During the analysis, I monitored the displacements and the deformation shape of the paper but I did not see distinguishable wavelengths, so I cannot support this.

Doug Coffin

In the testing we did, we did match up the wavelengths.

Artem Kulachenko

During testing did you measure the wavelengths, were you able to reproduce no CD constraint condition? Or did you have some CD constraints?

Doug Coffin

There was some friction, but the effect is very small.

Artem Kulachenko

The friction, as I showed you, might significantly affect the fluting problem, but in the printing press, this is not the case. Also we are aware of some research made for paper and we compared our computational results to those and they matched. In that case they also studied fluting with slow drying, moisturizing, but the wavelength was consistently higher than usually observed.

Patrice Mangin

May I take my Chairman's prerogative to make a comment which might be of interest to your work. About 2 years ago in a pressroom we were actually testing the Fujiwara (reference 2 in the paper) model that requires inked and non-inked areas. The pressman kept saying to me that he did not need that to get fluting. What we did was basically to print four colours, 100% solid on top of one another, making sure that even the nip where the plate joins together would be inked and, as expected by the pressmen, we got wonderful fluting. By the way, as we had very high ink coverage: may I thank you for your contribution to ink solidification. The fluting remained actually for months afterwards.

Another comment and also a question related to the temperature effect. We did actually look at the effect of dryer temperature and whether fluting would occur. We were very surprised that at 50°C, that is the temperature of the web going out of the dryer, there was never any fluting. Can you account for that in your model?

Artem Kulachenko

Yes, it can be explained with the last model that we have just shown because, in this model, we have a quite sharp bifurcation point, so we might expect that this phenomenon would not occur if we do not have sufficient strain variations. So the applied drying temperature might affect this variation and if that is not enough, we will not see any fluting. I am quite sure if you just ran the paper without any solids, you would still see this phenomenon.

Hannu Lepomäki   Metso Paper Inc

We have also studied a lot of fluting in Metso Paper with our customers. It is quite obvious that many process parameters related to running the papermaking line have effects on fluting. For example, we have found some correlation between headbox hydraulics and fluting as well as between press section draws and fluting. In papermaking lines as well as printing houses there are very many details affecting fluting. All of those need to be adjusted before getting any significant improvement.

I am interested to know how you will proceed in your research. As concerns microstructure, will you do some experiments in your laboratory or will you study real production lines? What will be your approach?

Artem Kulachenko

We are collaborating with SCA Research in developing the experimental procedure to identify the cause of strain variations, so we are very much involved with this.